

Phonon scattering at silicon crystal surfaces

Tom Klitsner* and R. O. Pohl

Laboratory of Atomic and Solid State Physics, Cornell University, Ithaca, New York 14853-2501

(Received 8 April 1987)

We have studied phonon scattering by films of metals, nonmetals, and condensed gases, 2 Å to 10^4 Å thick, deposited onto polished faces of Si crystals, through measurements of the thermal conductivity of these crystals in the boundary scattering regime, between 0.05 and 2.0 K. No evidence has been found for scattering by interface states or individual atoms or molecules adsorbed at the surface. Phonons are, however, strongly scattered by thin, discontinuous films and also by thick continuous ones, independent of the type of bonding to the substrate. Scattering by the islands of discontinuous thin films, or by microscopic disorder like grain boundaries, voids, or surface roughness in the thicker films can explain the observations. The model we develop to explain our findings is based on that for scattering by rough surfaces. Our experiments indicate that the high degree of disorder on the length scale of several hundred Å is not restricted to evaporated films, but also occurs in thermally grown oxide layers, Ni silicide films grown by surface reaction and even in layers of boron-ion-implanted silicon. It is concluded that thermal phonons in the frequency regime of 10–100 GHz (quantum energies 10^{-5} to 10^{-4} eV, corresponding to measuring temperatures 0.1 to 1.0 K) are very sensitive probes of surface film perfection on the submicrometer length scale.

I. INTRODUCTION

In dielectric solids, heat is carried by phonons. Their thermally excited frequency spectrum covers a broad range, but since the peak frequency of this spectrum increases in linear proportion with the temperature, measurements of the temperature dependent thermal conductivity can be used to probe a wide frequency range of phonons, and their interactions.

As tunable sources of monochromatic phonons have become available, with which phonons with frequencies in the terahertz regime have been generated, phonon spectroscopy with a high-frequency resolution has become another promising tool for the study of condensed matter.^{1–3} A problem encountered with such monochromatic sources and detectors in the frequency range above 100 GHz has been the poor efficiency of phonon transmission into and out of the substrate. Trumpp and Eisenmenger,⁴ for example, found an optimum yield of only 12% for 280-GHz phonons generated and detected with tin tunnel junctions deposited onto a polished silicon crystal. The strong phonon scattering demonstrated by these experiments not only limits the usefulness of these external phonon generators and detectors, but is also of more general importance, as in the case of heat transport across interfaces. In pursuing this problem, Eisenmenger and his collaborators also found that 280-GHz phonons in silicon were scattered at free, polished surfaces,^{4,5} and Wyatt and Page⁶ and Weber *et al.*⁷ reported evidence for phonon scattering at the interface between solids and liquid helium or adsorbed helium films which was traced to surface imperfections.⁷ As possible causes for the phonon scattering, motional degrees of freedom were suggested, such as tunneling states of adsorbates or surface defects,^{8–10} although clear evi-

dence for the existence of these excitations is still lacking.

Phonon scattering at crystal surfaces has also been observed in thermal conductivity measurements in the boundary scattering regime. Scattering at rough surfaces is well known, and is usually referred to as Casimir scattering.¹¹ Hurst and Frankl¹² and Campisi and Frankl¹³ have reported that Ar⁺-ion bombardment of a polished Si crystal, and oxidation of a polished Ge crystal also led to phonon scattering detected with thermal conductivity measurements; their temperature range of measurement was 1.5–4.0 K. Pohl and Stritzker¹⁴ studied the effect of Xe⁺-ion implantation on polished Al₂O₃ in the temperature range 0.07–2.0 K. They also observed that thin (≤ 100 Å average thickness) gold films caused phonon scattering. Removal of the gold film restored the phonon specularly of the polished surface. They showed that for the thin gold film to scatter the majority of the thermal phonons, a scattering process far stronger than that observed in the bulk of amorphous solids was required. Even in structurally fully disordered, amorphous solids the average phonon mean free path at, say, 1 K is of the order of 10^5 Å,¹⁵ yet gold films of less than 100-Å thickness caused nearly complete diffuse scattering of all incident phonons. The same argument was made for the thin ion implanted layer, which was also only a few hundred angstroms thick. These observations demonstrated that whatever defects caused such strong phonon scattering at the surfaces either had to have a very high number density, or a large scattering cross section, relative to known phonon scattering defects in the bulk.

The present study was undertaken in order to identify these scattering centers. Some of our results have been published previously,^{16,17} and will be reviewed only briefly, in order to complete the account.

II. EXPERIMENTAL TECHNIQUES

The substrates for the films were *p*-type (very lightly boron-doped) Si single crystals, $5 \times 0.5 \times 0.5 \text{ cm}^3$, kindly provided by Dr. V. Narayanamurti from AT&T Bell Laboratories. They had been cut from two boules of Wacker float-zone-refined material, with room temperature electrical resistivities of 627 and 900 $\Omega \text{ cm}$. Heat flow was along the $\langle 111 \rangle$ direction, and the faces were $\langle 211 \rangle$ and $\langle 110 \rangle$. Sample faces were polished at the AT&T Bell Laboratories Allentown Facility with 10- μm alumina, etched in 35% KOH at 90°C for 10 min, and then Syton polished (a suspension of colloidal $\alpha\text{-SiO}_2$ with particle size $\sim 300 \text{ \AA}$). Samples were occasionally repolished with Syton, especially when removing a film. After polishing, the samples were cleaned for about 30 min at 85°C in a 5:1:1 (by volume) solution of distilled H_2O , 30% H_2O_2 , and 30% NH_4OH . They were then rinsed thoroughly in distilled water, and stored in distilled water until just before they were to be used. Though this cleaning procedure is simple, it is extremely important not to deviate from it. To illustrate this point, Fig. 1 shows the effect of dipping a clean crystal (prepared as described above) into 48% HF, in an attempt to remove the native oxide layer. Clearly, this process caused diffuse scattering. That it was not caused by a roughening of the surface was suggested by the fact that subsequent cleaning as described above, completely removed the additional scattering. We therefore believe that this HF treatment led to the formation of adsorbates. How these adsorbates lead to phonon scattering will be explored in this paper.

The thermal conductivity measurements were performed in a dilution refrigerator, using a calibrated Ge

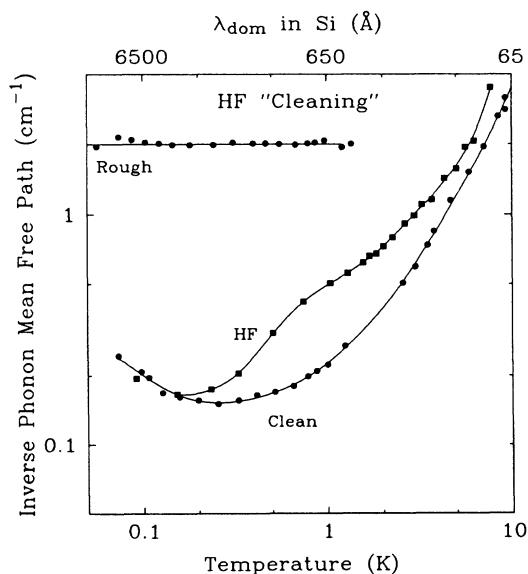


FIG. 1. The effect of briefly immersing a polished, clean silicon sample into concentrated HF. The increase of the inverse phonon mean free path over that for the polished, clean sample (lowest curve) indicates an increase in diffuse phonon scattering. The phonon mean free path is defined in Eq. (3).

thermometer as a standard which was checked against superconducting fixpoints at 98.76 mK, 162.2 mK, 205.05 mK, 515 mK, 844 mK, and 1.174 K. Indium-faced clamps were used to attach the heaters and thermometers, and each had a contact area of $2 \times (15 \text{ mm}^2)$. These clamps were always placed in the same way along the crystal, 3 cm apart. For the experiments with condensed gas films, the contact area of each clamp was $2 \times (1 \text{ mm}^2)$.

The *ex situ* (i.e., outside the cryostat) produced films were usually deposited in an oil-free, ion pumped electron beam evaporator, whose base pressure was 1×10^{-7} torr (films deposited in an oil pumped, 5×10^{-6} torr vacuum gave less reproducible results). Films of both strongly adhering (chemisorbed) materials, like Al, and of weakly adhering (physisorbed) materials, like Au, were prepared by this method. During deposition ($\sim 1 \text{ \AA/sec}$) the sample was rotated at 20 rpm, and its temperature was 300 K. Thickness was determined with a crystal thickness monitor. Rutherford backscattering (RBS), performed at the RBS Facility of the Cornell University Materials Science Center (MSC), was used to check the film thickness as well as uniformity and the absence of diffusion into the substrate. Electron micrographs were taken with a scanning electron microscope (JEOL JSM35) with a resolution of 60 \AA , at the Electron Microscope Facility of the MSC. Pictures of Au films as thin as 20 \AA (average thickness) could be imaged. The bare Si surface showed no detail, probably due to lack of contrast.

Silicon oxide films were grown in a wet-vapor oven at 900°C. They displayed a rainbow of colors, indicating nonuniformity of thickness on the length scale of centimeters. The 1500- \AA Ni silicide film was grown by heating a 1000- \AA Ni film in a vacuum furnace at 295°C at 2×10^{-8} torr for 1 h.

For the ion-implantation studies, B^+ ions were implanted at 100 keV on all four sides of the Si crystals, simultaneously exposing two of the sample faces which were inclined 45° relative to the ion beam. Total ion fluences for the two crystals were 3.6×10^{15} and 1.5×10^{16} per cm^2 of sample surface, respectively. Calculated peak concentration occurred at a depth of 0.21 μm , with a full width at half-concentration of 0.1 μm .¹⁸ Within this 0.1- μm range, boron concentration was 0.7 and 2.8 at. %, respectively.

The *in situ* deposition of gas films has been outlined before.¹⁷ Some additional information will be given here. A porous Vycor tube surrounded the Si crystal and the film thickness monitor (see Fig. 1 of Ref. 17). The thermal link of the tube was provided by 40 cm of 0.75-mm diameter copper wire attached to the ^4He pot of the refrigerator. After evacuating the cryostat at 300 K for ~ 10 h, the gas to be condensed (~ 0.5 atm) was admitted. Cooling the cryostat to helium temperature was done slowly (~ 5 h) in order to allow the major portion of the gas to condense into the Vycor tube (surface area of pores $\sim 10^4 \text{ m}^2$). Gas deposition was made by heating the Vycor tube slowly to ~ 8 K, while the sample stage was kept at either 1 or 4 K. The thickness of the *in situ* prepared gas films was determined by measuring the rel-

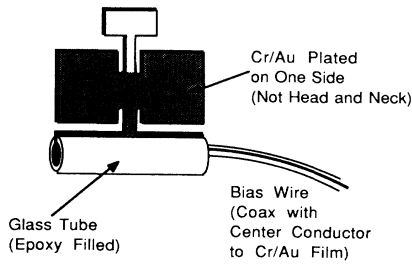


FIG. 2. Double torsional oscillator. In the antisymmetric mode, the small "head" and the larger "wings" (wing span 2 cm) move 180° out of phase around the axis of symmetry. A thin Cr layer makes the Au stick better. The bias voltage (~ 100 V dc) enhances the oscillatory amplitude. The oscillator is epoxied into a slotted glass tube, which in turn is clamped to the sample holder. Gas is deposited on one side of the oscillator.

ative change of period, $\Delta p/p$, of the antisymmetric torsional mode of the double oscillator shown in Fig. 2, following a design developed by Kleiman *et al.*¹⁹ The oscillator was micromachined out of 18-mil thick, 5–15- Ω cm resistivity Si wafers with faces perpendicular to $\langle 100 \rangle$, using photolithographic techniques and an anisotropic chemical etch (a mixture of ethylenediamine, pyrocatechol, and water, for short EDP, described in Refs. 20 and 21). Excitation and detection was done capacitively with counter electrodes. Resonant condition was maintained by a phase-locked loop.

The quality factor Q was found to peak around 3 K at a value of $Q \sim 6 \times 10^6$, see Fig. 3, top, but then decreased to 0.75×10^6 , as the temperature was lowered to 0.1 K (the reason for this drop is not known). Although the period p was temperature dependent below 5 K, Fig. 3,

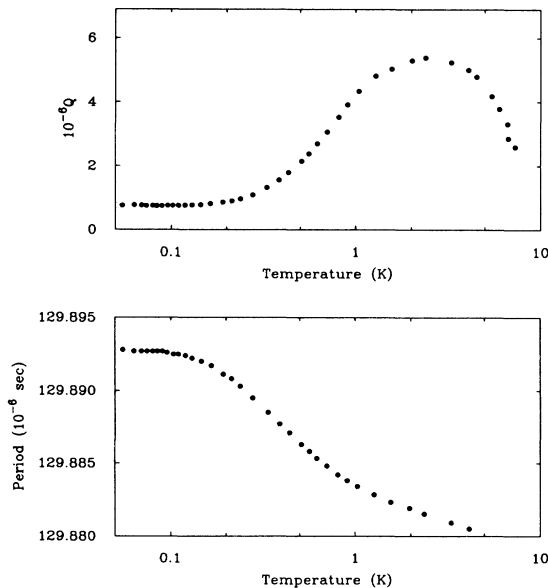


FIG. 3. Temperature dependence of the quality factor Q (top) and of the period (bottom) of the torsional oscillator of Fig. 2.

bottom, it could be kept stable to within 1 part in 10^8 over several hours or even days by controlling the temperature, or to within 1 part in 10^9 over tens of minutes, for 10-sec integration times.

Since the shear moduli of the adsorbed gases are small compared with that of silicon, the change in period during a deposition is determined almost entirely by the mass of the adsorbed gases, and can be approximated by

$$\frac{\Delta p}{p} = 2 \frac{t_{\text{gas}} \rho_{\text{gas}}}{t_{\text{Si}} \rho_{\text{Si}}}, \quad (1)$$

where t is the thickness, and ρ the mass density (of the gas film or the silicon, respectively). Thus, one monolayer of Ne corresponds to a change $\Delta p/p$ of about 1 part in 10^7 , and one can detect changes of 0.01 monolayer.

Adsorbed gases also change the Q of the torsional oscillator, see Fig. 4. However, since the effect was small in the temperature range available to us, we did not investigate the origin of this effect any further.

We did, however, use the oscillator as a sensitive pressure gauge by monitoring the change in resonant frequency over a measured period of time to determine the rate at which residual gas molecules were plating out onto the oscillator. This rate was turned into a partial pressure for the adsorbing gases. For a sticking coefficient of 1 (a reasonable assumption at these temperatures) and from simple kinetic considerations, the time to form a monolayer is given by²²

$$t_{\text{monolayer}} = \frac{(2\pi m_i k_B T)^{1/2}}{P_i d^2}, \quad (2)$$

where P_i is the partial pressure of the gas, d is the mean

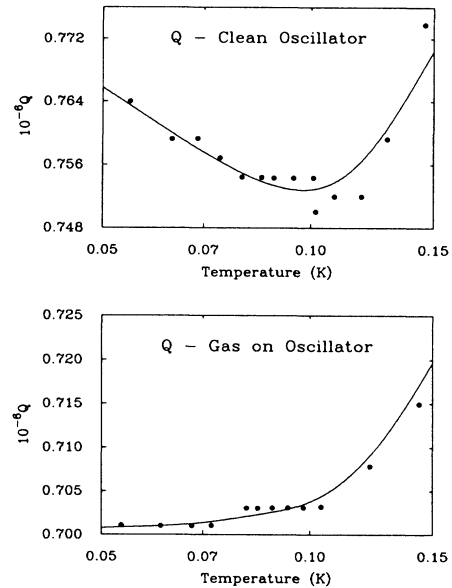


FIG. 4. Influence of a $1\text{-}\mu\text{m}$ -thick Ne film on the low-temperature quality factor. Above 0.15 K, the onset of the peak in Q (Fig. 3, top) quickly obscures this relatively small effect.

diameter of the gas molecules (in general $\sim 3 \text{ \AA}$), m_i is the mass of a gas molecule, T is the temperature, and k_B is Boltzmann's constant.

We observed no change in the resonant frequency of the oscillator to a part in 10^8 over a period of about

$$P_{\text{Ne}} = \frac{[2\pi(3.3 \times 10^{-26} \text{ kg})(1.381 \times 10^{-23} \text{ J/K})(0.1 \text{ K})]^{1/2}}{(3 \times 10^6 \text{ s})(3 \times 10^{-10} \text{ m})^2} = 2 \times 10^{-12} \text{ N/m}^2 = 1.5 \times 10^{-14} \text{ torr}.$$

(This value supersedes the one quoted previously.¹⁷) It represents an upper limit, since we actually saw no change in the frequency of the oscillator within the limits of its stability. This is a very impressive vacuum, especially when one compares it to the best vacua obtained in room-temperature UHV chambers, which are $\geq 10^{-12} \text{ Torr}$.

For describing the thermal conductivity Λ , we will use the familiar and simple expression

$$\Lambda = \frac{1}{3} C v l, \quad (3)$$

where C is the specific heat, v an appropriate average over the speeds of sound²³ close to the Debye speed of sound, and l is the average phonon mean free path. For Si, based on elastic measurements,²³ $C = 5.91 \times 10^{-7} T^3 \text{ J K}^{-4} \text{ cm}^{-3}$, $v = 5.66 \times 10^5 \text{ cm s}^{-1}$. From specific heat measurements,^{24,12} $C = 6.02 \times 10^{-7} T^3 \text{ (J K}^{-4} \text{ cm}^{-3})$ (from which $v_D = 5.93 \times 10^5 \text{ cm s}^{-1}$, and $\Theta_D = 648 \text{ K}$ are determined); we will use this value of C in Eq. (3).

In relating measuring temperature to phonon frequency, we will use the dominant phonon approximation, in which it is assumed that at any temperature the heat is carried predominantly by phonons of a single frequency. If we choose those phonons which contribute most to

three days ($3 \times 10^5 \text{ sec}$), while the oscillator was kept at about 0.1 K. A change of frequency of 1 part in 10^8 corresponds to about a monolayer of H_2 or D_2 , and about a tenth of a monolayer of Ne [from Eq. (1)]. We thus obtained from Eq. (2) for Ne

the specific heat at that temperature, then in the Debye approximation their frequency is related to T through $h \nu_{\text{max}} = 3.83 k_B T$, where h and k_B have the usual meaning. Thus, 1 K corresponds to 80 GHz. By comparing the location T_0 of low-temperature resonance dips in the thermal conductivity, with the resonance frequency causing them, we had found previously²⁵ $h \nu_0 = 4.25 k_B T_0$, an insignificant difference. As in the past (e.g., Ref. 15), we will use this relation to define the dominant phonon frequency ν_{dom} :

$$\nu_{\text{dom}} = 4.25 (k_B / h) T = (90 \text{ GHz K}^{-1}) T. \quad (4)$$

The dominant phonon wavelength λ_{dom} is defined as $\lambda_{\text{dom}} = (v / \nu_{\text{dom}})$. In Si, $\lambda_{\text{dom}} = 650 \text{ \AA}$ at 1 K. For some of the other substances used as surface films in this study, λ_{dom} at 1 K, determined with the help of the Debye speed of sound, are listed in Table I.

III. EXPERIMENTAL RESULTS AND DISCUSSION

At temperatures below the thermal conductivity maximum in high purity crystals (10 K for silicon), the heat flow is determined largely by phonon collisions at the crystal surfaces, and not by bulk scattering. The lowest curve in Fig. 5 was measured (only below 2 K) on a sample with rough (sandblasted) surfaces, the uppermost curve on a sample with polished and cleaned surfaces. Thin metal films evaporated onto such surfaces lead to a reduction of the thermal conductivity, as shown for three films of different thicknesses. However, there is a threshold temperature below which this diffuse scattering vanishes; this threshold shifts to lower temperatures as the average film thickness increases.

It is easier to inspect these data when they are presented as the inverse average phonon mean free path, l^{-1} , defined by Eq. (3). l^{-1} is proportional to the scattering rate, $\tau^{-1} = v l^{-1}$, and in the following will also be referred to as such. When the sample has rough surfaces, l^{-1} is temperature independent and agrees well with the Casimir prediction,¹¹ see Fig. 6. For the polished, clean surface, l^{-1} is over ten times smaller but shows some temperature dependence. Above 1.0 K, l^{-1} increases rapidly with increasing temperature. At 1 K, most of the heat is carried by phonons with frequencies $\nu_{\text{dom}} = 90 \text{ GHz}$. At 3 K, $\nu_{\text{dom}} = 270 \text{ GHz}$. Monochromatic phonons with $\nu = 270 \text{ GHz}$ have been found to scatter at silicon crystal surfaces treated similarly to those used here, while 90-GHz phonons were found to be mostly specularly reflected.²⁶ Our thermal conductivi-

TABLE I. Low-temperature Debye speed of sound v_D for some of the solids used in this study, and their rounded off dominant phonon wavelengths λ_{dom} at 1 K, calculated with the help of v_D as described in the text.

Material	v_D (10^5 cm s^{-1})	$\lambda_{\text{dom}, 1 \text{ K}}$ (\AA)
Si ^a	5.93	650
α -SiO ₂ ^b	4.1	450
NaCl ^c	3.84	420
Al ^d	3.42	370
Ag ^d	1.96	200
Au ^d	1.46	160
H ₂ ^e	1.27	140
D ₂ ^e	1.16	125
Ne ^f	0.71	75 ^g

^aReference 52.

^bSee Ref. 15.

^cReference 53.

^dReference 54.

^eReference 55.

^fReference 56.

^gIn Ref. 17, we suggested 70 \AA . The value given here, although insignificantly different, is closer to the correct value.

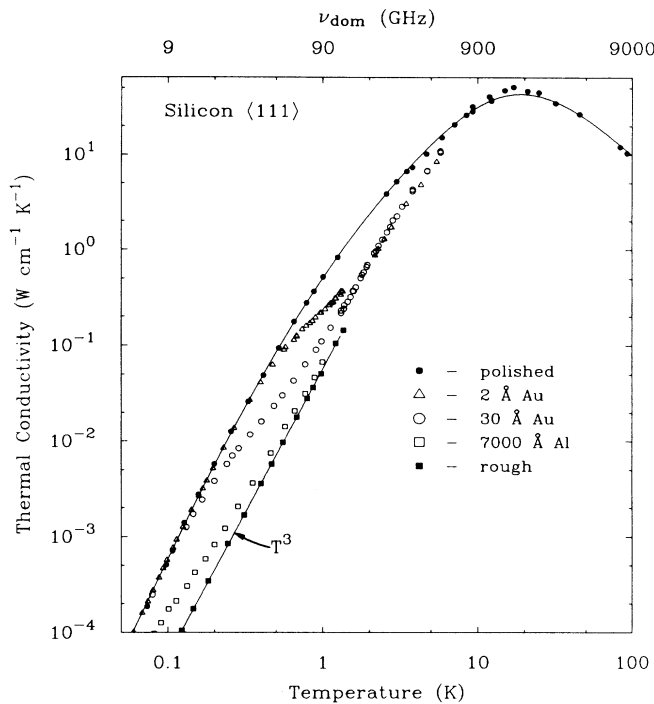


FIG. 5. Thermal conductivity of a pure silicon single crystal with different surface treatments. Top curve: Syton polished and cleaned; bottom: sandblasted. The intermediate curves were measured after metal films were deposited (*ex situ*) onto the polished and cleaned surfaces.

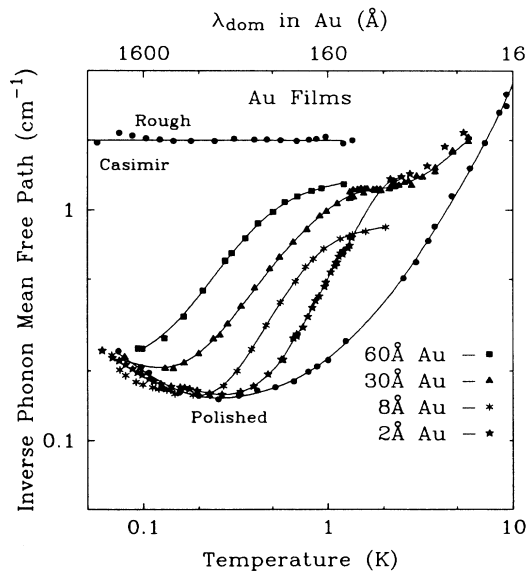


FIG. 6. Diffuse scattering by Au films deposited *ex situ* on a polished Si substrate. The inverse mean free path for the sandblasted (rough) sample agrees with the Casimir prediction, including phonon focusing, for heat flow in the $\langle 111 \rangle$ direction in Si.

ty measurements confirm these findings.

We found the perfection of the surfaces to be highly reproducible, i.e., we obtained the same $l^{-1}(T)$ after the same surface preparation, as long as we did not change the geometry, i.e., sample dimension as well as position and contact area of the clamps used to attach heaters and thermometers. In the absence of significant phonon scattering in the bulk and at the surface, any clamps attached to the sample have an important influence on the radiative phonon flow.²⁷ We are thus, strictly speaking, not measuring thermal conductivity, but a geometry-dependent thermal conductance. This distinction is important only for quantitative analyses. Details will be discussed elsewhere.²⁸

We must also mention the increase of l^{-1} below 0.3 K. Previously,¹⁷ we believed this increase, too, to be a geometrical effect of the radiative heat flow, but it now appears²⁸ more likely to be caused by phonon resonant scattering by the boron trace impurities,²⁹ with a concentration of $\sim 10^{14} \text{ cm}^{-3}$. Because of its reproducibility within the same batch of silicon single crystal samples, this low-temperature rise of l^{-1} can also be viewed simply as part of the baseline for this experiment. For the present investigation, all that matters is that we found our clean, polished samples to yield reproducible results and to be highly specular for phonons with frequencies less than 100 GHz.

Figure 6 also illustrates the phonon scattering by gold films and its dependence on the film thickness. Scattering is noticeable even for submonolayer average thickness, and increases continuously with increasing thickness. The transition from predominantly specular reflection to diffuse scattering as the temperature increases (the threshold temperature), is also clearly seen. This transition moves to lower temperatures as the film thickness increases. Above the threshold temperature

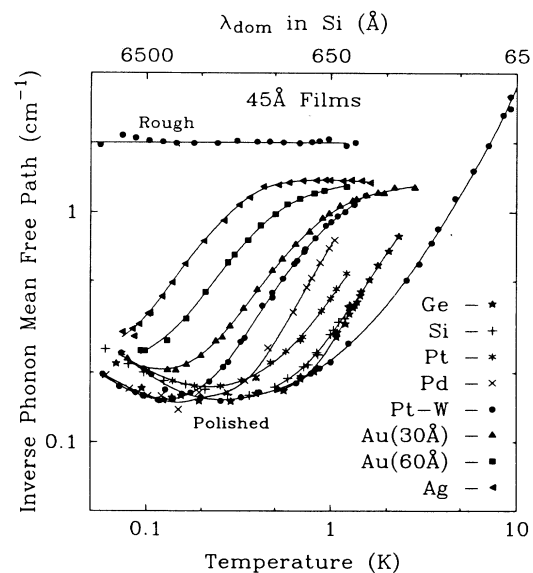


FIG. 7. Scattering from $\sim 45\text{-}\text{\AA}$ films of various materials. Scattering increases with the degree of expected film roughness.

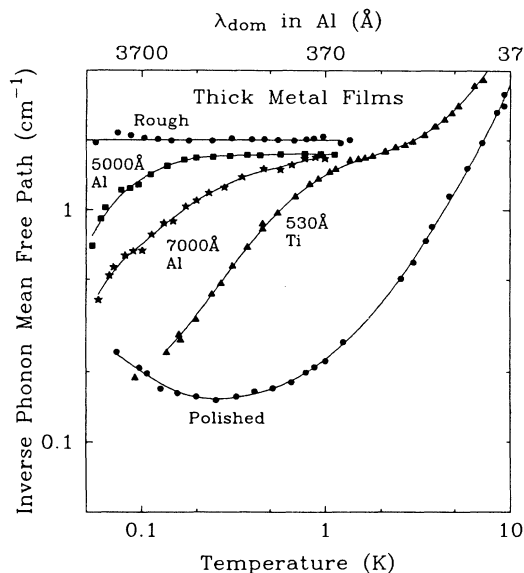


FIG. 8. Scattering from thick films of Al and Ti.

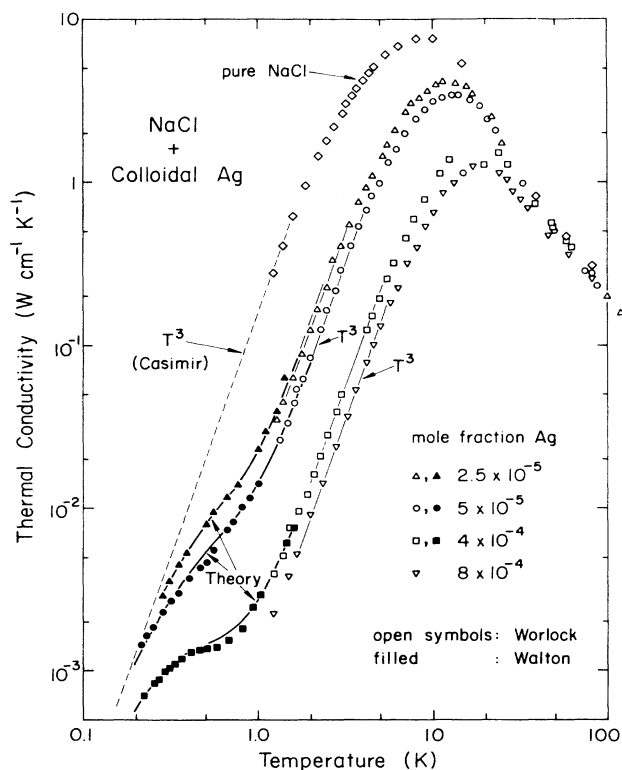


FIG. 9. Thermal conductivity of NaCl single crystals containing colloidal Ag particles. From Worlock (Ref. 30) and Walton (Ref. 31). The straight lines drawn through Worlock's data were calculated assuming geometric scattering by particles with a characteristic particle size (diameter) of (from top to bottom) 55, 72, 100, and 120 Å. The curves drawn through Walton's data were calculated assuming the scatterers to be Ag spheres of diameter $2r = 100; 108, 128$ Å (the highest mole fraction sample was not measured by Walton). Thus, elastic scattering by microscopic (spherical) particles seems to describe the data between 0.2 and 5 K very well.

the inverse mean free path l^{-1} approaches a constant value which appears to be somewhat smaller than the Casimir value. Qualitatively the same scattering is observed when other metals, or even nonmetals, are evaporated onto clean, polished Si surfaces, as shown in Fig. 7, where the film thickness is kept fairly constant (45 Å). The threshold temperature appears to depend on the material. For thicker metal films, see Fig. 8, phonon scattering occurs almost over the entire temperature range, i.e., the threshold temperature shifts towards the low-temperature end of the range of our measurements. The data in Figs. 6–8 show that the type of bonding is relatively unimportant for the phonon scattering. Au, Ag, and Pt are physisorbed and can easily be rubbed off, while Al, Ti, Ge, and Si are chemisorbed and are very strongly adhering. This is the first indication that the scattering is not caused by motional states of individual atoms adsorbed at the surface, since the energy of those states and their coupling to the phonons should be very sensitive to the bonding.

What may cause the scattering, and specifically how can the threshold be explained? A qualitatively similar scattering rate, i.e., one which sets in rather abruptly as the temperature increases, and then approaches a constant value, is known for crystals containing microscopic inclusions in the bulk. In Figs. 9 and 10, we show measurements by Worlock and Walton of the thermal conductivity of sodium chloride single crystals containing small amounts of colloidal silver.^{30,31} Below 0.2 K, l^{-1} approaches the Casimir limit (all samples had rough sur-

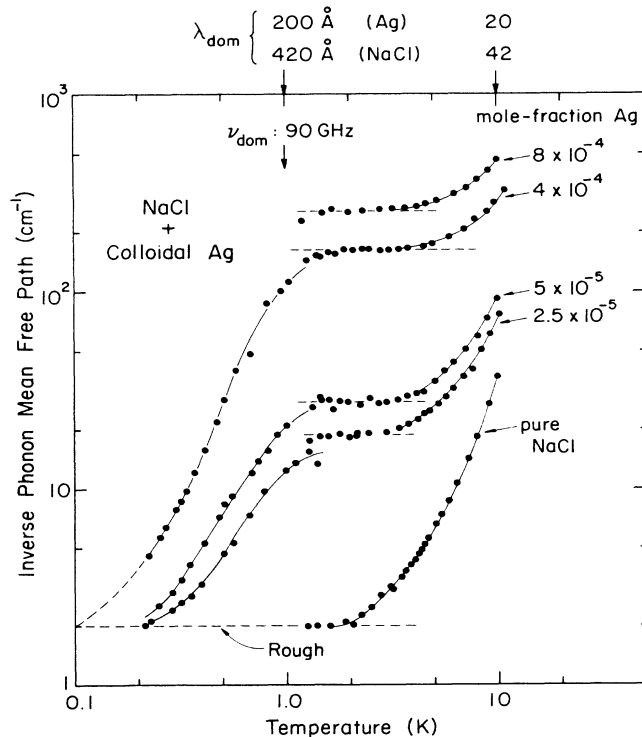


FIG. 10. Phonon scattering in NaCl with Ag colloids (data as in Fig. 9). Since the scattering occurs in the bulk, the scattering rates are in excess of the Casimir rate.

faces). As the temperature increases, the scattering rate rises rapidly and approaches a constant value around ~ 1 K. Worlock used these plateau values of l^{-1} to determine the sizes and number densities of the colloidal silver particles, assuming they were spherical and scattered the phonons with their geometrical cross section. He found particle diameters $2r$ of the order of 100 Å (details in the caption of Fig. 9). Elastic scattering by a sphere should be geometrical for wavelengths λ such that

$$(2\pi/\lambda)r \gg 1, \quad (5)$$

and should follow a Rayleigh law, $\propto \nu^4$, for

$$(2\pi/\lambda)r \ll 1. \quad (6)$$

The dominant phonon wavelength for NaCl is 420 Å at 1 K (see top scale in Fig. 10), thus a rapid drop of the phonon scattering rate was to be expected below 1 K, and was indeed found by Walton.³¹ The heavy solid curves in Fig. 9 are his computed thermal conductivities, with particle radii (and with them the particle number densities, since the total amount of silver was known) as adjustable parameters. From his best fits, he determined radii only slightly larger than the ones determined by Worlock from the measurements above 1 K, see caption of Fig. 9, thus confirming the picture of elastic phonon scattering by microscopic particles. In the transition region between Rayleigh scattering and geometric scattering, i.e., for $(2\pi/\lambda)r \approx 1$, resonant scattering can lead to peaks in the scattering cross section, depending on the acoustic properties of host and inclusion.^{31,32} Resonant scattering would lead to a peak in l^{-1} ; this was not observed in NaCl:Ag, in agreement with Walton's calculation of the scattering cross section in this particular case.³¹

The scattering rate (or l^{-1}) observed for colloidal particles shows much similarity to that found here for metal films on polished surfaces, except that the latter cannot lead to a scattering in excess of the Casimir scattering, while such an upper bound for the scattering in the bulk does not exist. A connection between the scattering by colloids in the bulk and by films on top of the polished surfaces suggests itself when these films are viewed under the electron microscope. Thin metal films tend to be discontinuous, forming an islandlike structure which covers most of the surface. The 60-Å-thick gold film (thermal conductivity measurements in Figs. 5 and 6) showed an average island size of ~ 400 -Å diameter, while the 30-Å film showed ~ 200 -Å diameter islands. It is suggestive that these islands will also lead to an elastic scattering of a wave impinging on them, somewhat like the colloidal particles in the bulk. We can use the threshold temperatures observed for the gold islands to estimate their dimensions, through a comparison with the threshold temperature observed in NaCl:Ag, and the known colloid radii. We arbitrarily define as the threshold temperature T_{th} the temperature at which l^{-1} has dropped to one half its plateau value. For the Ag colloids, T_{th} is thus determined as ≈ 0.8 K, as seen in Fig. 10. At 0.8 K, $\lambda_{dom} = (420 \text{ Å})/0.8 = 525 \text{ Å}$ in NaCl. As

average value of the colloid diameters, we choose $2r = 100 \text{ Å}$. Thus, $(2\pi/\lambda)r = 1.2 \approx 1$, which merely means that we picked a reasonable definition for T_{th} . For the 60-Å Au film, T_{th} by the same definition is determined to be 0.3 K, and for the 30-Å film, 0.5 K; see Fig. 6. For these temperatures, λ_{dom} in silicon is 2200 and 1300 Å, respectively. From these values we determine a characteristic dimension d of the scattering islands, defined as $d = \lambda_{dom}/2\pi$, to be $d = 350 \text{ Å}$ and 200 Å , respectively, close to the island diameter determined with the electron microscope. One may wonder whether the characteristic dimension in this case should be the diameter or, as in the case of the colloid scattering, the radius, or some other length involving the thickness of the islands, and also, how the elastic properties of the island might affect the answer. Nonetheless, the close agreement between d and the island diameter, and in particular its shift in proportion with it, supports this picture of the phonon scattering.

We were unable to measure the island size of the thinnest Au films with the scanning electron microscope, because the reflected electron beams were too weak. Based on the observation that the threshold temperatures for the 8 and 2 Å films were approximately two and four times larger than for the 30-Å-thick film, we would estimate island sizes of $(200 \text{ Å})/2 = 100 \text{ Å}$ and $(200 \text{ Å})/4 = 50 \text{ Å}$, respectively, as a first application of phonons for a spectroscopic investigation of a surface film. Electron microscope pictures of very thin gold films on silicon oxide substrates or other substrates do exist from other investigators (see, for example, Refs. 33 and 34). The structures, however, depend much on details of the film preparation, and thus these measurements of island size cannot be applied to our films.

Although this model used to describe the phonon scattering by the discontinuous island is intuitively appealing, it has several shortcomings. For example, how does an elastic wave couple to an essentially flat island attached to the polished substrate, or specifically, how can a wave in the short-wavelength limit [Eq. (5)] be diffusely scattered at the flat interface? Another question is raised by the observation that even thick and certainly continuous films have been found to scatter phonons, as shown in Fig. 8; in Fig. 11 a 300-Å-thick Au film scatters about as strongly as the 60-Å film. If we believed that thick films, which appear like mirrors to the eye, were indeed structurally highly perfect, their effect on the phonons would present a major puzzle. It is well known, however, that such films are always highly nonuniform on the length scale between 10^2 and 10^4 Å. They contain grain boundaries, voids and void networks, dislocations, and even their surfaces show what is called cauliflowerlike roughness which increases with increasing film thickness.³⁵⁻³⁷ As a specific example of the surface roughness we refer to a recent tunneling microscope study of 10^3 -Å-thick Au films on glass, which showed a waviness on the scale of $\sim 10^2$ Å (period and amplitude).³⁸ Electron micrographs of our own thicker films ($> 10^2$ Å) showed many cracks, forming the well-known "mud flat" structure: A 150-Å-thick film had cracks separated by $\sim 10^3$ Å. In films that were even

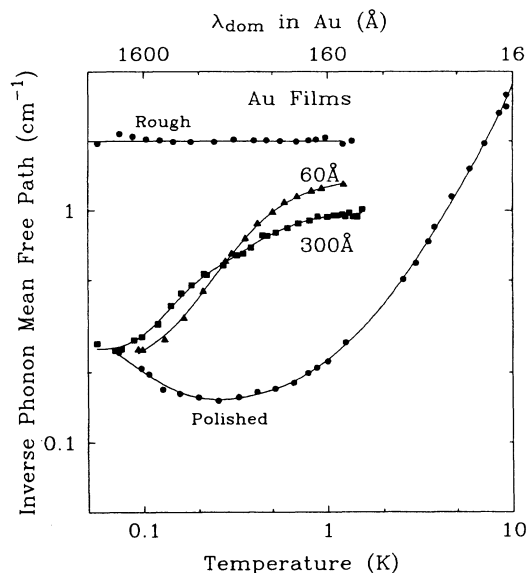


FIG. 11. Comparison of scattering from a discontinuous 60-Å (average) Au film and from a smoother, more continuous 300-Å Au film. Note the flatter profile for the thicker film, and the crossing of the two curves at ~ 300 mK.

thicker (~ 500 Å), no cracks could be detected with the electron microscope.

In order to understand the scattering in these cases, we will now show that it is better not to start from the picture of some foreign matter residing on the substrate, but rather from a rough surface of the substrate itself. The fact that this roughness is caused by some foreign matter residing on the polished substrate will be included as a refinement. Twersky³⁹ has treated the case of scattering and reflection by rough surfaces by considering random distributions of hemispheric protuberances of radius r on a base plane. He calculated the reflections coefficient and the scattering cross section per unit area, σ , and found for $(2\pi/\lambda)r \ll 1$, that σ varies as λ^{-4} , as in Rayleigh scattering, and has a strong dependence on r ($\propto r^6$). For $(2\pi/\lambda)r \gg 1$, σ is essentially geometrical and wavelength independent. The crossover from Rayleigh to geometric scattering occurs for $(2\pi/\lambda)r \sim 1$. Thus, surface irregularities alone, without differences in the elastic properties, can lead to phonon scattering similar to that caused by inclusions in the bulk. For a refinement of the scattering theory, including the effect of surface waves, we refer to the work by Shiren⁴⁰ and Nakayama.⁴¹ In order to apply this theory to our thick films, all we need to do is view their disorder as a more complicated "roughness" caused by the external as well as the internal surfaces between grain boundaries, voids, etc. (A discussion of the scattering of hypersound by grain boundaries in metal films has recently been presented by Weis and co-workers.⁴²)

In order for all the thermal phonons to be scattered within a thick film, their mean free path must be of the order of the film thickness or less, i.e., of the order of hundreds of angstroms in our cases (see Figs. 8 and 11).

Although such a mean free path is much shorter than that in amorphous solids in our temperature range,¹⁴ mean free paths of this order have indeed recently been observed in very fine grained bulk crystalline solids. As examples we mention polycrystalline natural shale and welded tuff.⁴³ In these rocks, phonon mean free paths of a few hundred angstroms have been observed in thermal conductivity experiments below 1 K. Grain sizes in these samples were of the order of 10^4 Å, and hence lamellar structures within the grains, which were identified as phonon scatterers in several other minerals,⁴⁴ were suggested as the source of the scattering. The microstructure in thick evaporated films is of the order of the film thicknesses or less³⁵⁻³⁷ and thus can explain the phonon scattering we have observed in our thick films. Similar microstructure is to be expected in the large islands of discontinuous films, and can thus explain the scattering of the short-wavelength phonons we mentioned above. In the continuous films, the occurrence of a threshold in the scattering rate is an indication of a certain correlation length of the disorder; phonons with wavelengths exceeding this correlation length are scattered less.

In order to make this picture of the phonon scattering more realistic, we will now include the variation of the elastic properties between substrate and film. This step will be aided through an experimental study of thin films of Ne, H₂, and D₂ that have been deposited *in situ* at low temperatures onto the polished surfaces.¹⁷ The very large differences between the elastic properties of these solids and those of the substrate, and the high reproducibility of the low-temperature deposition of these films made this choice very attractive. All three condensed gases lead to phonon scattering, although the effects are different. Since the data for Ne and H₂ have been published before¹⁷ they will only be reviewed briefly; some of the data are reproduced for the convenience of the reader.

Ne, deposited onto a substrate held at 1 K, see Fig. 12, leads to noticeable scattering rates even for films of an average thickness as small as 1 Å, and $l^{-1}(T)$ shows a threshold temperature T_{th} which shifts from ~ 1 K to ~ 0.2 K as the film thickness grows to 70 Å. Even above T_{th} , in the temperature-independent region, l^{-1} does not approach the Casimir limit. For H₂, see Fig. 13, scattering becomes measurable only when the average thickness exceeds 100 Å. The scattering is observable over the entire temperature range, without evidence of a threshold, independent of the deposition temperature. For Ne, the threshold is suppressed when the film is deposited while the substrate is held at 4 K (the highest temperature at which the gas was found to stick).¹⁷ For D₂ films, effects intermediate between those of Ne and H₂ were found. Measurable effects on the scattering require a thickness of several tens of angstroms, see Fig. 14, if the D₂ film is deposited at 4 K, and no scattering threshold is observed. At a deposition temperature of 1 K, however, a threshold may or may not occur, as shown in Fig. 15, and the scattering is stronger. We see that a 30-Å film produces more scattering than the 70-Å film deposited at 4 K, though

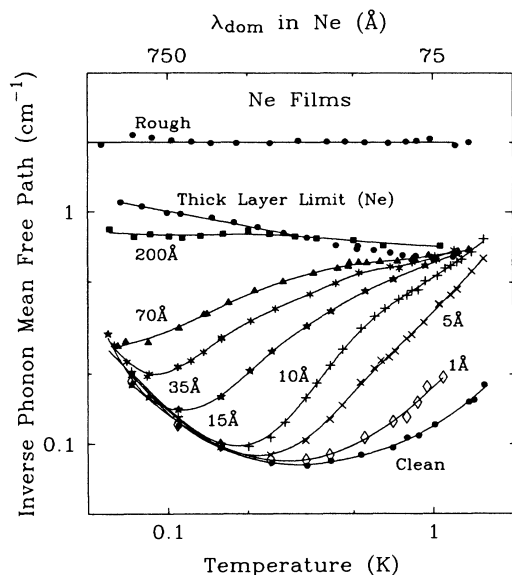


FIG. 12. Diffuse scattering rates for different coverages of Ne on Si held at 1 K during the deposition. Even submonolayer coverage (average thickness) leads to a noticeable enhancement of the diffuse scattering. The scattering then increases continuously with increasing coverage until it reaches the thick layer limit. Above this coverage, the scattering becomes independent of the thickness. The transition from specular reflection to diffuse scattering as the temperature increases is clearly visible for all coverages.

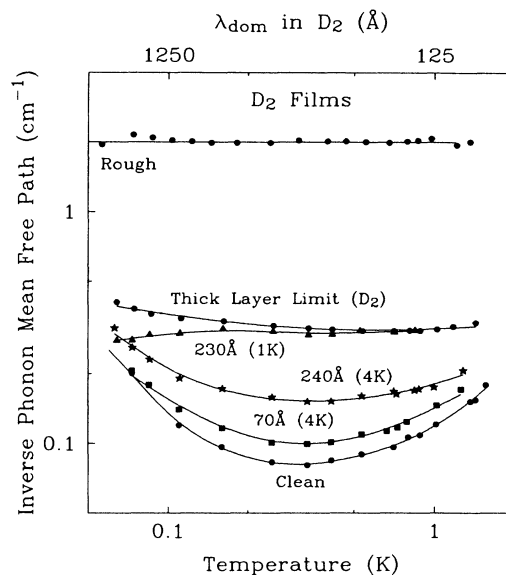


FIG. 14. Comparison of D₂ films deposited on the substrate at 1 and 4 K: 70 Å (4 K), 240 Å (4 K), 230 Å (1 K).

there is still no threshold. However, the subsequently deposited 40-Å film causes a clearly visible threshold, similar to that produced by the Ne films.

Quantitative evidence that the waves are scattered in the adsorbed films, and not at the interface, is obtained from the observation that with increasing film thickness the scattering rate approaches a saturation value beyond which l^{-1} does not increase, no matter how thick the film is (we studied films up to 10^4 Å thick). This so-called thick layer limit is actually a rather small scatter-

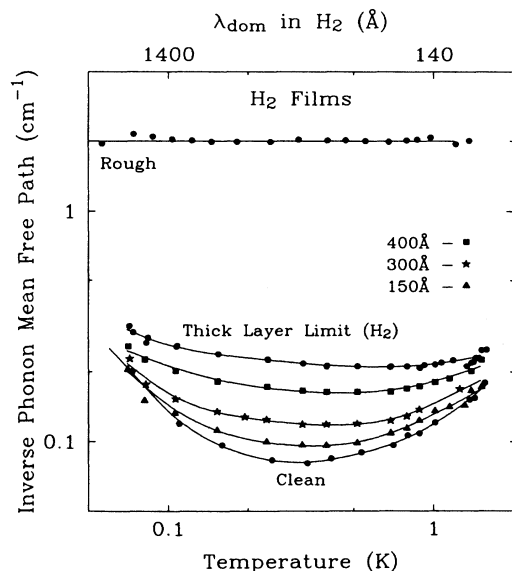


FIG. 13. Diffuse scattering rates for different coverages of H₂ on Si held at 1 K during the deposition. No scattering is observed for coverages below one hundred angstroms. Note also the absence of a threshold in the scattering, in contrast to that observed for Ne. In the thick layer scattering limit the probability for specular reflection is still high, $\sim 95\%$ (Ref. 28).

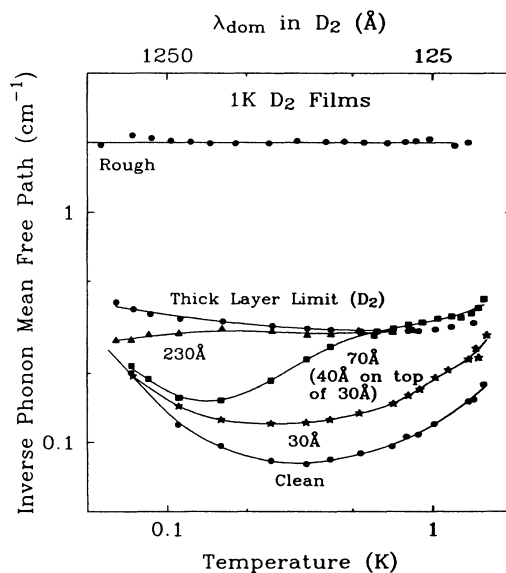


FIG. 15. D₂ films deposited on the substrate at 1 K. Note that the profile can have either a sharp threshold or it can be fairly flat. The 70-Å film was produced by depositing a 40-Å film on top of the 30-Å film.

ing rate for H_2 and even for D_2 (compare the thick layer mean free path with the Casimir mean free path). We have previously suggested¹⁷ that this large residual reflectivity is caused by the large acoustic mismatch between the hard silicon and the soft condensed gas films. The phonons which cannot enter the softer medium because of this mismatch, are specularly reflected at the interface. In the thick layer limit, all phonons entering the film will be scattered. We have modeled this process using a Monte Carlo calculation which will be described in detail elsewhere,²⁸ and have calculated the heat flow, and from that l^{-1} . The calculation neglected phonon focusing and assumed the acoustic properties of the films to be those of the bulk solids.⁴⁵ The arrows on the right of Fig. 16 show the results, which include the scattering rate measured at 1 K for the clean sample. They correspond to an angularly averaged specularity of 98% for H_2 , 95% for D_2 , and 85% for Ne, or a probability for entering the condensed gas films of $\approx 2\%$, 5%, and 15%, respectively. The close agreement between these calculated and the observed values of l^{-1} for the three films, Fig. 16, strongly supports our suggestion as expressed in Ref. 17.

These results have identified the role played by the interface; it limits, through acoustic mismatch, the fraction of the phonons entering the film, while specularly reflecting the rest. Diffuse scattering at the interface is negligible. Those phonons that enter the film, can be scattered. If the film is continuous, they may be scattered by its disorder, voids, grain boundaries, surface

roughness, and the like, as suggested above. If the film is discontinuous, acoustic mismatch will also limit the fraction of the phonons that may be scattered by the islands. Such a penetration of the wave is obviously also contained in the theory of scattering by colloidal inclusions in the bulk. It enters into this theory through the elastic properties of host and inclusion.^{31,32}

In analogy to the scattering by colloidal inclusions in the bulk as well as by surface roughness, we expect the transition from Rayleigh to geometric scattering to occur when the phonon wavelength is of a magnitude comparable to that of the island dimension. Since in the picture we are using now the wave actually has to enter the island in order to be scattered, it seems more appropriate to consider the wavelength λ_i within the island, rather than in the substrate. The dominant λ_i at 1 K for the various films we have studied are listed in Table I, their temperature dependences are indicated on the upper abscissae of several of the figures. In the absence of a more quantitative model, we shall assume that the transition from Rayleigh to geometric scattering occurs when $\lambda_i = d$, where d is the island diameter. We test this assumption through a comparison with the data obtained on the thin gold films (Fig. 6). For the 60-Å film, $T_{th} = 0.3$ K, thus $\lambda_i = 320$ Å. This is close to the average island diameter, which is ~ 400 Å in this case. Obviously such an agreement can only be called encouraging, and must not be viewed as a proof of our naive scattering model. However, a further refinement of the scattering model must wait until measurements on more carefully controlled islands can be performed. These efforts are presently underway. The strength of our present model lies in the fact that it is equally applicable, at least in a qualitative way, to all films we have studied, whether they are discontinuous and thin, or continuous and thick, regardless of their material, and of the mode of preparation. The following examples will help to make this point.

Compare the scattering rates in Ne films (deposited at 1 K), Fig. 12, with those in Au films, Fig. 6. The scattering rates are remarkably similar for the two substances, and thus we conclude that the film structures are very similar. From the threshold temperatures, we can estimate the Ne island sizes d . For the 10-Å film, for example, we observe $T_{th} = 0.5$ K, thus $\lambda_i = 150$ Å = d . Films of H_2 , on the other hand, show no scattering threshold. We conclude that the disorder in these films has a spread of correlation lengths which extends beyond 10^3 Å, which is the longest phonon wavelength in solid H_2 used in our experiments. The disorder is also somewhat less than in the Ne films: In H_2 , all phonons transmitted into the film will be scattered if the film thickness exceeds 400 Å, while in Ne, a layer ~ 200 Å thick is enough. We also notice that a Ne film deposited onto 4-K substrates does not exhibit a threshold and appears to be smoother than the films deposited at 1 K, since it scatters less. The disorder in D_2 films is apparently more difficult to control. These observations, although only qualitative at this time, demonstrate the potential of our technique as an analytic tool for the study of the microstructure of films on surfaces.

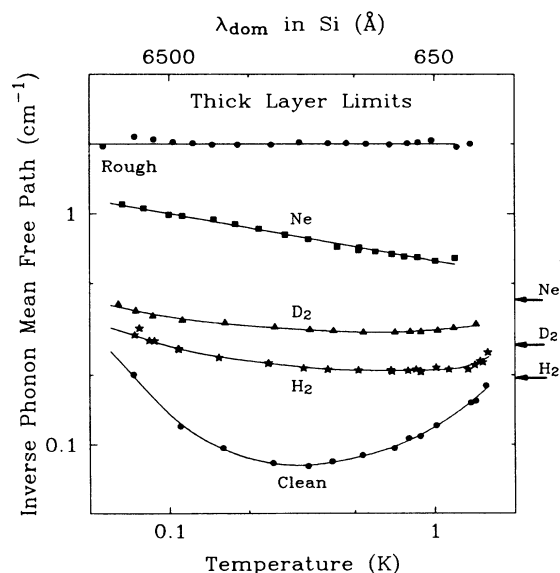


FIG. 16. Thick layer maximum scattering limits for condensed gas films of Ne, D_2 and H_2 . Films up to 10^4 Å thick were studied, Ref. 17. Arrows on the side indicate the value of l^{-1} expected on the basis of acoustic mismatch between Si and these condensed gases for isotropic angles of incidence, and correspond to a probability for specular reflection of 98% for H_2 , 95% for D_2 , and 85% for Ne (Monte Carlo calculation by Fischer, details in Ref. 28).

A closer inspection of the phonon scattering in the gold and in the neon films does indeed reveal some differences. First, the scattering rate in the Ne increases monotonically with film thickness, Fig. 12, while that in the Au films shows a less regular behavior, Figs. 6 and 11. It is known that the microstructure of Au films depends strongly on the conditions of deposition and subsequent handling.³³ One of the reasons for doing the *in situ* deposition experiments was that we expected that they could lead to far more reproducible microstructures in the films. The measured scattering rates appear to bear out this difference, consistent with the picture that the scattering in the films is indeed caused by their microstructure.

The second difference is that in the thick layer limit, the scattering in Au is not determined by the acoustic mismatch, which would predict that $\sim 90\%$ of the phonons would enter the Au film, where they may be scattered by the disorder in the film. Yet, the data above T_{th} indicate a much higher reflectivity, somewhere around 50%. For the thin, discontinuous films, this high reflectivity could result from partial coverage by the Au islands, an argument which, however, cannot be invoked for the 300-Å film. Conceivably, a physisorbed Au film does not fully adhere over the entire surface area it covers. Note that for the chemisorbed films (e.g., Al, Fig. 8), the thick layer limit is very much closer to the Casimir limit, and is in better agreement with the high transmission coefficient ($> 95\%$) calculated from acoustic mismatch.

Figure 17 shows the scattering by evaporated silicon films on a polished Si substrate. It takes relatively thick films to produce diffuse scattering; a threshold is observed. These films are likely to be amorphous, yet they must have some weak, long-range disorder to which the thermal phonons are sensitive above the threshold temperature of each film. The two thickest Si films (500 and

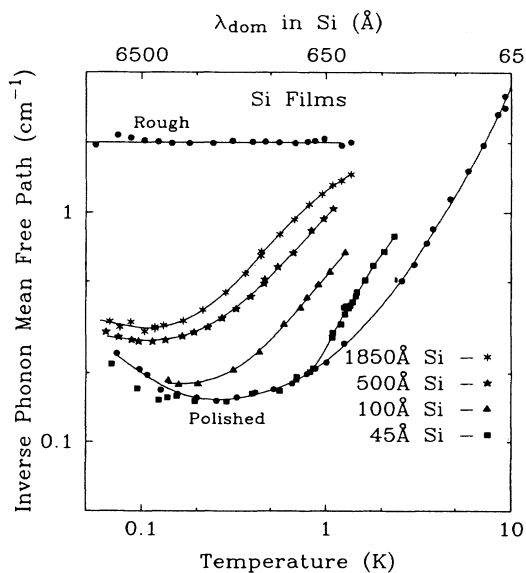


FIG. 17. Diffuse scattering by Si films on a polished Si substrate.

1850 Å) show rather similar scattering. This suggests that the thicker film is less disordered (per volume) than the thinner one. This is another example of the poor reproducibility of the structural quality of *ex situ* produced films.

A freshly deposited 300 Å thick silver film, Fig. 18, shows the scattering characteristic for islands. After aging for some time, the film has obviously changed, and the correlation length of the disorder has spread out. Electron micrographs and Rutherford backscattering analysis showed that the Ag had acquired substantial amounts of impurities, predominantly sulfur, chlorine, and bromine. Apparently, the reaction products made the film more irregular.

Silicon dioxide films that have been thermally grown on Si are known to be continuous. Yet, these films also scatter diffusely (Fig. 19) even though this requires relatively thick films. An approximately 1600-Å-thick film causes an inverse mean free path l^{-1} [defined in Eq. (3)] of about 0.7 cm^{-1} at 1 K (note that specular reflection at the interface can be ignored because of the small acoustic mismatch in this case). Compared to $l_{\text{Casimir}}^{-1} = 2 \text{ cm}^{-1}$, it follows that $\sim 30\%$ of the incident phonons are scattered as they move through the film and back, a total of 3200 Å, corresponding to a phonon mean free path of $\sim 10^4 \text{ Å}$ in the film. In bulk $\alpha\text{-SiO}_2$, the mean free path at this temperature exceeds 10^5 Å . We conclude that even this presumably highly uniform film has a remarkable degree of disorder on the length scale of the thermal phonon wavelength at this temperature. This disorder can be within the film, or at its interface or its outer surface, as waviness or roughness. In the latter case, the surface or interface disorder would have to increase with increasing film thickness. This is conceivable, considering the diffusion process by which the film grows. A 1500 Å Ni-silicide film grown on Si showed

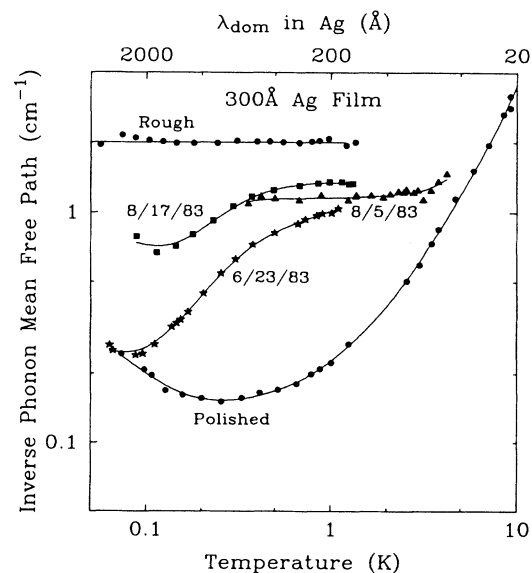


FIG. 18. Aging of a 300-Å Ag film. The scattering strength at low temperatures increases with age (the dates of measurement are listed next to the curves).

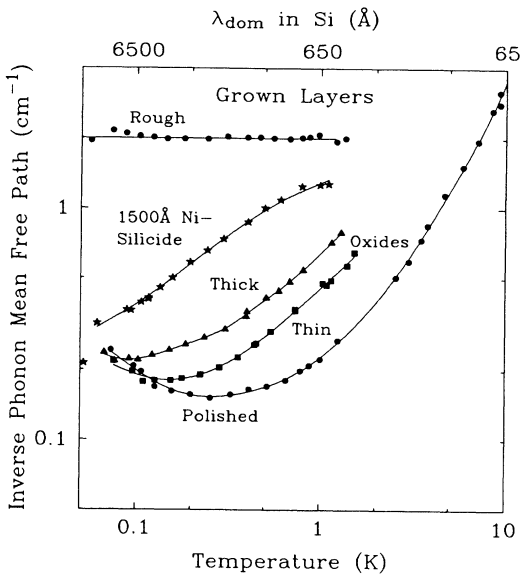


FIG. 19. Scattering from layers grown onto the Si substrate. Thin silicon oxide: $< 1000 \text{ \AA}$; thick: $1200\text{--}2000 \text{ \AA}$, as judged by the range of colors (deep purple to goldish) indicating varying thicknesses, with an average thickness of $\sim 1600 \text{ \AA}$. The $< 1000\text{-\AA}$ film also showed thickness variations. The Ni-silicide was prepared by reacting a Ni film with the substrate.

more scattering, i.e., was even more disordered on the scale of the thermal phonon wavelengths than the silicon oxide films.

Destructive interference (stopbands) in the transmission of monochromatic phonons ($200\text{--}400 \text{ GHz}$) through an approximately 700 \AA thick superlattice of amorphous SiO_2 and Si produced by electron beam evaporation has been observed at 1 K .⁴⁶ This proved that at least part of the phonon beam was not scattered as it moved through the thin films. Our experiments on films of these materials (Figs. 17 and 19) confirm this qualitative observation. At $\sim 2 \text{ K}$ ($\nu_{\text{dom}} = 200 \text{ GHz}$), films of similar total thickness scatter $\sim 50\%$ of the incident phonons. For a quantitative comparison, details of the stopband line shape would be needed. Even at 4 K ($\sim 400 \text{ GHz}$), which is beyond our range of measurement, we expect, by extrapolation, that some of the phonons will still be specularly reflected, i.e., will not be scattered in these films.

The various thin film materials studied differ greatly in their bonding strength to the substrate. Yet, the scattering is little affected by this difference. Compare, for example, the scattering in the (strongly bonded) silicon oxide with that in the (weakly bonded) H_2 . Even if we would ignore the fact that it takes hundreds of monolayers to cause significant scattering in both substances, the mere fact that the bonding has practically no influence on the scattering is clearly incompatible with the picture that the scattering results from individual adsorbed atoms at the interface, since their impurity modes (e.g., tunneling states) would depend greatly on their bonding to the substrate.

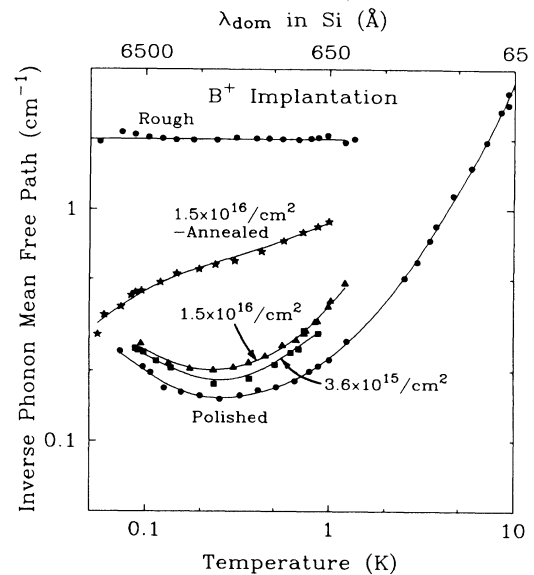


FIG. 20. Scattering by B^+ ion implanted into a thin surface layer (depth $\sim 3000 \text{ \AA}$, deposition energy $\sim 100 \text{ keV}$), see text, Sec. II.

It would be interesting to measure the scattering of films prepared under more highly controlled conditions resulting in better films. Highly perfect films produced by molecular-beam epitaxy should not scatter at all.

B^+ -ion implantation also leads to diffuse scattering, see Fig. 20. Obviously, no islands or films are formed in this process, but it is known that a layer several thousand angstroms thick is severely disordered, as de-

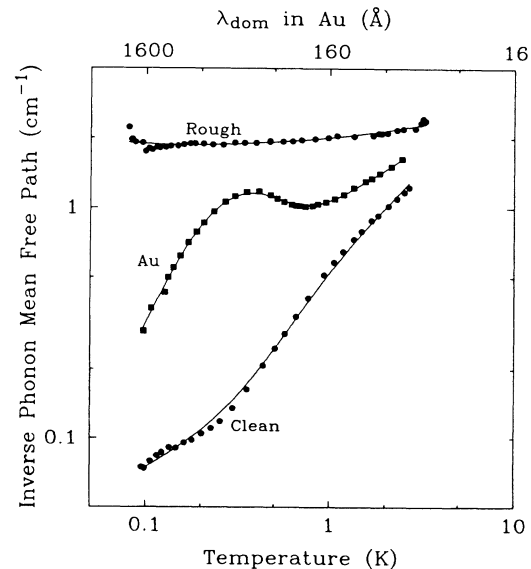


FIG. 21. Our only observation of resonant scattering by a surface film. A $\sim 20\text{-\AA}$ -thick Au film was deposited on a cylindrical (as seed pulled by Wacker Chemie, $800\text{-}\Omega\text{-cm}$) silicon crystal in an oil-pumped vacuum ($P_{\text{min}} = 5 \times 10^{-6} \text{ Torr}$). The structure of the film is unknown.

scribed in Sec. II. The diffuse scattering occurs over the entire temperature range, somewhat as in adsorbed hydrogen films.¹⁵ The relatively weak disorder appears to have a wide spread in correlation lengths. Annealing the sample at 700°C leads to bulk scattering through diffusion of impurities, determined as such by its insensitivity to a surface polish.

Elastic scattering by a microscopic particle may or may not lead to resonant scattering, depending on the elastic properties of particle and host, as emphasized by Walton³¹ for the case of Ag colloids in NaCl. Not to find a resonance in thermal conductivity experiments, however, does not necessarily prove the absence of a resonance. Conceivably, the resonance may simply be masked because of a broad range of resonant frequencies resulting, for example, from a wide distribution of particle (or island) sizes. In the course of this investigation, we have indeed once found evidence of resonant scattering. A 20-Å Au film produced a resonance at ~400 mK (36 GHz), Fig. 21. This observation suggests that thin, discontinuous films can lead to resonant scattering, the condition for its occurrence, however, are not yet known.

IV. CONCLUSIONS

Polished silicon surfaces are highly specular for thermal phonons below 1 K, i.e., for phonons of frequency of 90 GHz and below. Such phonons are, however, extremely sensitive to films of adsorbed matter, even to very thin ones. The bonding between substrate and film plays a remarkably small role in the scattering, and there is no evidence, that for the phonon frequencies of these experiments, atoms or molecules adsorbed directly to the surface act as phonon scatterers. Rather, the scattering occurs predominantly within the films, and is caused by their microscopic disorder. The transmission into the films is governed by acoustic mismatch. The disorder in the film depends on the material and on the conditions under which it was deposited.

One of the simplest cases is that of discrete islands. Elastic scattering, comparable to that by protuberances on the surface of the crystal, can provide a good picture for understanding the magnitude and temperature dependence of the scattering. Rayleigh scattering occurs for long wavelengths, and geometric scattering for short wavelengths. For the latter, the scattering cross sections are equal to the geometric ones, and this explains why an extremely thin discontinuous film can lead to such strong phonon scattering, which was the puzzling observation that originally attracted our attention to the phonon scattering by very thin films.¹⁴ Resonant scattering, which can occur when a normal mode of the island resonates with the phonons, has been seen only once. The reason why we have not observed it more frequently may be a spread of the resonant frequencies in the films produced by our technique for sample preparation.

Scattering is also observed in thick, continuous films. Apparently, the disorder known to exist in these films and on their free surfaces leads to the strong scattering. As an example, even the least disordered films, which

appear to be those produced by oxidizing the silicon substrate, cause a scattering rate at 1 K which is over 10 times larger than in bulk silica. In this case, the possibility of interface roughness as a source of the scattering needs also to be considered. Long-range disorder also arises in ion implanted thin layers.

The great scattering strength of thin, discontinuous, and even of continuous films, which has been established through this investigation, has important implications for the preparation of specularly reflecting surfaces and of high-quality films for acoustic work. Furthermore, any attempts at identifying other scattering centers at crystal surfaces, such as localized modes or tunneling states, will have to be carried out with great caution, lest their effect be masked by accidental thin layers consisting of small islands or other nonuniform coverages. We remind the reader of the effect of a brief HF etch shown in Fig. 1 which apparently caused surface contamination.

Since microscopic surface defects have now been identified as such efficient scattering centers, one may wish to explore whether they, rather than surface defects on the atomic scale postulated previously, may have been responsible for earlier observations of diffuse scattering. We will give a few examples.

Even for our polished, clean surfaces, there is an abrupt upturn of l^{-1} as T increases above 0.5 K, as observed at the onset of a threshold. Assume that this increase is caused largely by residual surface roughness or adsorbed "dirt," with a correlation length or with island sizes of the order of a few tens of angstroms. This would lead to a threshold temperature T_{th} of a few K. Now, let us look how these postulated islands may have shown up in earlier studies: In phonon pulse experiments at low temperature, it has been found that longitudinal phonons are not transmitted across an interface as readily as transverse phonons.⁴⁷⁻⁵⁰ Since the longitudinal waves always have a higher velocity than the transverse ones (by a factor of ~2), their $\lambda_{dom,l}$ are always larger than the transverse $\lambda_{dom,tr}$. It follows from our picture that for a given film, the threshold temperature T_{th} between specular reflection and diffuse scattering will be higher for the longitudinal waves by the same factor. Buechner and Maris⁴⁹ have investigated the heat transport between Si and solid H₂ for heat pulse temperatures between 1.5 and 8 K, while more recently, Kinder *et al.*⁵⁰ have studied the Kapitza resistance between superfluid ⁴He and Si for heat pulse temperatures less than 2.2 K. At the higher temperatures (> 2 K), both groups found that there was anomalous (i.e., greater than acoustic mismatch) phonon transmission across the interface, presumably due to surface imperfections. As the phonon temperature was lowered, the longitudinal mode coupled across the interface less and less—i.e., it coupled to surface impurities less and less—until, at the lowest temperatures, all anomalous coupling vanished. The data of Buechner and Maris⁴⁹ also showed the same behavior for the transverse waves, *but at a lower temperature than for longitudinal waves* (< 1.5 K). These observations agree qualitatively with our assumption of extended surface defects. At high phonon temperatures

(10 to 20 K) Swannenburg and Wolter⁵¹ found the transmission coefficients from Si into liquid ⁴He to be equal for both longitudinal and transverse modes. (Kinder *et al.*⁵⁰ indicate that they have confirmed these results at high phonon temperatures). Since in this case the phonon temperature is well above the threshold temperature for both modes, we would indeed expect both modes to couple equally well to the surface layers. These examples must suffice. A systematic search for such macroscopic defects coupled with a study of their effects on the phonon scattering is necessary to test our conjecture.

ACKNOWLEDGMENTS

We thank J. E. VanCleve, H. E. Fischer, S. Gregory, J. P. Sethna, N. S. Shiren, and E. T. Swartz for many

helpful discussions, and H. E. Fischer in particular for performing the Monte Carlo simulation calculations shown in Fig. 16. We also thank J. D. Reppy and P. L. Gammel for help with the torsional oscillator, J. W. Mayer for the use of the Rutherford-backscattering equipment, V. Narayanamurti for supplying the high-purity Si samples, and M. Meissner for his assistance during the early stages of the experiment. The micro-machining of the torsional silicon oscillator and the ion implantations were made possible through the National Research and Resource Facility for Sub-micron Structures; we thank M. J. Skvarla for his expert help. An equipment grant from the AT&T Foundation is gratefully acknowledged. This work was supported by the National Science Foundation through the Cornell University Materials Science Center.

*Present address: AT&T Bell Laboratories, Murray Hill, NJ 07974-2070.

¹Phonon Scattering in Condensed Matter V, edited by A. C. Anderson and J. P. Wolfe (Springer-Verlag, Berlin, 1986).

²Phonon Scattering in Condensed Matter, edited by W. Eisenmenger, K. Lassmann, and S. Döttinger (Springer-Verlag, Berlin, 1984).

³Phonon Scattering in Condensed Matter, edited by H. J. Maris (Plenum, New York, 1980).

⁴H. J. Trumpp and W. Eisenmenger, Z. Phys. B **28**, 159 (1977).

⁵D. Marx and W. Eisenmenger, Z. Phys. B **48**, 277 (1982).

⁶A. F. G. Wyatt and G. J. Page, J. Phys. C **11**, 4927 (1978).

⁷J. Weber, W. Sandmann, W. Dietsche, and H. Kinder, Phys. Rev. Lett. **40**, 1469 (1978).

⁸T. Nakayama, J. Phys. C **10**, 3273 (1977).

⁹H. Kinder, Physica **107B**, 549 (1981).

¹⁰H. Kinder and K. Weiss, in *Phonon Scattering in Condensed Matter V*, Ref. 1, p. 218; H. Kinder, A. de Ninno, D. Goodstein, G. Paternó, F. Scaramuzzi, and D. Cunselo, *ibid.* p. 234.

¹¹H. B. G. Casimir, Physica **5**, 495 (1938).

¹²W. S. Hurst and D. R. Frankl, Phys. Rev. **186**, 801 (1969).

¹³G. J. Campisi and D. R. Frankl, Phys. Rev. B **10**, 2644 (1974).

¹⁴R. O. Pohl and B. Stritzker, Phys. Rev. B **25**, 3608 (1982).

¹⁵R. C. Zeller and R. O. Pohl, Phys. Rev. B **4**, 2029 (1971).

¹⁶Tom Klitsner and R. O. Pohl, in *Phonon Scattering in Condensed Matter*, Ref. 2, p. 188.

¹⁷Tom Klitsner and R. O. Pohl, Phys. Rev. B **34**, 6045 (1986); in *Phonon Scattering in Condensed Matter V*, Ref. 1, p. 162.

¹⁸J. F. Gibbons, W. F. Johnson, and S. W. Mylroie, *Projected Range Statistics, Semiconductors and Related Materials*, (Dowden, Hutchinson, and Roth, Stroudsburg, PA, 1975).

¹⁹R. N. Kleiman, G. K. Kaminsky, J. D. Reppy, R. Pindak, and D. J. Bishop, Rev. Sci. Instrum. **56**, 2088 (1985).

²⁰R. M. Finne and D. L. Klein, J. Electrochem. Soc. **114**, 965 (1967).

²¹A. Reisman, M. Berkenblit, S. A. Chan, F. B. Kaufman, and D. C. Green, J. Electrochem Soc. **126**, 1406 (1979).

²²*Methods of Experimental Physics*, Vol. 14 of *Vacuum Physics and Technology*, edited by G. L. Weissler and R. W. Carlson (Academic, New York, 1979).

²³A. K. McCurdy, H. J. Maris, and C. Elbaum, Phys. Rev. B **2**, 4077 (1970).

²⁴P. Flubacher, A. J. Leadbetter, and J. A. Morrison, Philos. Mag. **4**, 273 (1959).

²⁵R. O. Pohl, in *Elementary Excitations in Solids*, edited by G. F. Nardelli (Plenum, New York, 1969), p. 259.

²⁶S. Burger, W. Eisenmenger, and K. Lassmann, J. Low Temp. Phys. **61**, 401 (1985); see also the review by W. Eisenmenger, in *Phonon Scattering in Condensed Matter V*, Ref. 1, p. 204.

²⁷J. E. VanCleve, Tom Klitsner, and R. O. Pohl, in *Phonon Scattering in Condensed Matter V*, Ref. 1, p. 177.

²⁸Tom Klitsner, J. E. VanCleve, H. E. Fischer, and R. O. Pohl (unpublished).

²⁹A. Ambrosy, K. Lassmann, A. M. de Goër, B. Salce, and H. Zeile, in *Phonon Scattering in Condensed Matter*, Ref. 2, p. 361; A. M. de Goër, M. Locatelli, and K. Lassmann, J. Phys. (Paris) Colloq. **42**, C6-235 (1981).

³⁰J. M. Worlock, Phys. Rev. **147**, 636 (1966).

³¹D. Walton, Phys. Rev. **157**, 720 (1967); D. Walton and E. J. Lee, *ibid.* **157**, 724 (1967).

³²G. Johnson and Rohn Truell, J. Appl. Phys. **36**, 3466 (1965); as introduction see P. M. Morse and H. Feshbach, *Methods of Theoretical Physics* (McGraw-Hill, New York, 1953), p. 1483.

³³L. Bachmann and H. Hilbrand, *Basic Problems in Thin Films Physics* (Vandenhoeck and Rupprecht, Goettingen, 1966), p. 77; Th. Andersson and C. G. Granquist, J. Appl. Phys. **48**, 1673 (1977); V. D. Frechette, J. C. Pulver, and D. R. Rossington, J. Am. Ceram. Soc. **64**, 463 (1981); T. G. Andersson, J. Appl. Phys. **52**, 7212 (1981); P. M. Th. M. Van Attekum, P. H. Woerlee, G. C. Verkade, and A. A. M. Hoeben, Phys. Rev. B **29**, 645 (1984).

³⁴L. I. Maissel and R. Glang, *Handbook of Thin Film Technology* (McGraw-Hill, New York, 1983), Chap. 8.

³⁵B. A. Movchan and A. V. Demchishin, Phys. Met. Metallogr. (USSR) **28**, 83 (1969).

- ³⁶S. Nakahara, *Thin Solid Films* **45**, 421 (1977).
- ³⁷R. Messier, A. P. Giri, and R. A. Roy, *J. Vac. Sci. Technol. A* **2**, 500 (1984); R. Messier and J. E. Yehoda, *J. Appl. Phys.* **58**, 3739 (1985).
- ³⁸J. Schneir, R. Sonnenfeld, P. K. Hansma, and J. Tersoff, *Phys. Rev. B* **34**, 4979 (1986).
- ³⁹V. Twersky, *J. Acoust. Soc. Am.* **29**, 209 (1957).
- ⁴⁰N. S. Shiren, *Phys. Rev. Lett.* **47**, 1466 (1981), *J. Phys. (Paris) Colloq.* **42**, C6-816 (1981).
- ⁴¹T. Nakayama, *J. Phys. C* **18**, L667 (1985), *Phys. Rev. B* **32**, 778 (1985); **33**, 8664 (1986).
- ⁴²O. Weis, in *Phonon Scattering in Condensed Matter V*, Ref. 1, p. 381; B. Lehr, H. Ulrich, and O. Weis, *Z. Phys. B* **48**, 23 (1982).
- ⁴³R. O. Pohl and J. W. Vandersande, in *Scientific Basis for Nuclear Waste Management*, edited by D. G. Brookins (North-Holland, New York, 1983), p. 711.
- ⁴⁴J. W. Vandersande and R. O. Pohl, *Geophys. Res. Lett.* **9**, 820 (1982); J. W. Vandersande, P. N. Chopra, and R. O. Pohl, in *Phonon Scattering in Condensed Matter*, Ref. 2, p. 182.
- ⁴⁵C. L. Reynolds, Jr. and A. C. Anderson, *Phys. Rev. B* **14**, 4114 (1976).
- ⁴⁶O. Koblinger, J. Mebert, E. Dittrich, S. Dottinger, and W. Eisenmenger, in *Phonon Scattering in Condensed Matter V*, Ref. 1, p. 156; the first observation of a phonon stopband was reported by V. Narayanamurti, H. L. Stormer, M. A. Chin, A. C. Gossard, and W. Wiegmann, *Phys. Rev. Lett.* **43**, 2012 (1979) on a crystalline GaAs/Al_xGa_{1-x}As superlattice produced by molecular-beam epitaxy.
- ⁴⁷C.-J. Guo and H. J. Maris, *Phys. Rev. Lett.* **29**, 855 (1972); J. S. Buechner and H. J. Maris, *ibid.* **34**, 316 (1975).
- ⁴⁸R. E. Horstman and J. Wolter, *Phys. Lett.* **62A**, 279 (1977).
- ⁴⁹J. S. Buechner and H. J. Maris, *Phys. Rev. B* **14**, 269 (1976).
- ⁵⁰H. Kinder, A. De Ninno, D. Goodstein, G. Paternó, F. Scaramuzzi, and S. Cunsolo, *Phys. Rev. Lett.* **55**, 2441 (1985).
- ⁵¹T. J. B. Swannenburg and J. Wolter, *Phys. Rev. Lett.* **31**, 693 (1973).
- ⁵²H. J. McSkimin and P. Andreatch, *J. Appl. Phys.* **35**, 2161 (1964).
- ⁵³J. T. Lewis, A. Lehoczyk, and C. V. Briscoe, *Phys. Rev.* **161**, 877 (1967); see also Ref. 30.
- ⁵⁴G. Simmons and H. Wang, *Single Crystal Elastic and Aggregate Constants* (MIT Press, Cambridge, Mass., 1971).
- ⁵⁵R. Wanner and H. Meyer, *J. Low Temp. Phys.* **11**, 715 (1973).
- ⁵⁶R. Balzer, D. S. Kupperman, and R. O. Simmons, *Phys. Rev. B* **4**, 3636 (1971).